EXPERIMENTAL STUDIES ON THE ELECTRICAL PROPERTIES OF HIGH TEMPERATURE SUPERCONDUCTOR CABLE STRUCTURES

PROJECT REPORT

Submitted by

SAJANA A SAMAD

TKM20MEIR15

to

APJ Abdul Kalam Technological University
in partial fulfillment of the requirements for the award of
Master of Technology in Mechanical Engineering.
(Industrial Refrigeration and Cryogenic Engineering)

Department of Mechanical Engineering

TKM College of Engineering, Kollam

February 2022

DEPARTMENT OF MECHANICAL ENGINEERING

TKM COLLEGE OF ENGINEERING, KOLLAM

CERTIFICATE

Certified that this report entitled '*Experimental studies on the electrical properties of high temperature superconductor cable structures*' is the report of seminar presented by **SAJANA A SAMAD, TKM20MEIR15** during **2021-2022** in partial fulfillment of the requirements for the award of the Degree of Master of Technology in Mechanical Engineering (Industrial Refrigeration and Cryogenic Engineering) of APJ Abdul Kalam Technological University.

Guide: 7/7/22

Dr. K.E. Reby roy
Professor
Dept. of Mechanical Engineering
TKM College of Engineering, Kollam

Coordinator:

Dr. K.A Shafi
Professor
Dept. of Mechanical Engineering
TKM College of Engineering, Kollam

Dr. P.N.Dileep
Head of the Department
Dept. of Mechanical Engineering
TKM College of Engineering, Kollam

DECLARATION

I, SAJANA A SAMAD hereby declare that, this project report entitled **Experimental studies on the electrical properties of high temperature superconductor cable structures** is the bonafide work of mine carried out under the supervision of Dr. K. E. Reby Roy Professor, Dept. of Mechanical Engineering TKM College of Engineering, Kollam. I declare that, to the best of my knowledge, the work reported herein does not form part of any other project report or dissertation based on which a degree or award was conferred on an earlier occasion to any other candidate. The content of this report is not being presented by any other student to this or any other University for the award of a degree.

SAJANA A SAMAD

University Register No: TKM20MEIR15 of year 2020-2022

7/7/22

DR. K.E. REBY ROY

Professor

Dept. of Mechanical Engineering

TKM College of Engineering, Kollam

DR. P.N. DILEEP

Head, Department of Mechanical Engineering

TKM College of Engineering, Kollam

Date:07/07/2022

ACKNOWLEDGEMENTS

I take this opportunity to express my deep sense of gratitude and sincere thanks to all who helped us to complete the project successfully.

I am deeply indebted to my guide **Dr. K.E.Reby roy**, Professor, Department of Mechanical Engineering for his excellent guidance, positive criticism and valuable comments. I am greatly thankful to **Dr.P.N.Dileep**, Head of Mechanical Engineering Department for his support and cooperation.

Finally, I thank our parents and friends near and dear ones who directly and indirectly contributed to the successful completion of my project.

SAJANA A SAMAD

Place: Kollam

Date: 04/07/2022

ABSTRACT

The recent work deals with the experimental study of the alternating current losses on different structural arrangements of HTS cables. HTS cables with the various structural arrangement are studied for the AC losses at liquid nitrogen temperature(77K). Experiments are conducted on Roebel cable structures, CORC cable structures and Twisted stack cable structures. The experiment is done at the liquid nitrogen temperature. The investigation is carried out to study and compare the alternating current losses in the different structural arrangements. The effect of the various structural orientation is scrutinized. The result indicates that the CORC cable structure has very low alternating current losses while in the liquid nitrogen temperature. Findings show that the structural arrangements significantly affect the losses through the high-temperature superconducting cables. The structural arrangements significantly contribute to the passage of the current passing through the HTS cables.

Keywords : HTS cables, Roebel cables ,CORC cables, Twisted stack cables, AC losses

CONTENTS

LIST OF FIGURES

List of tables

ABBREVATIONS

HTS	**High temperature superconductor**
R_{in}	**Inner radius**
w_s	**Width of straight section**
w_c	**Width of cross over**
l_t	**Transposition length**
α	**Cross over angle**

CHAPTER 1

INTRODUCTION

Superconductivity is the property of some materials to conduct direct current (DC) electricity without energy loss when cooled under a temperature (referred to as Tc). Such materials also expel magnetic fields during their transition to the superconducting state. Superconductivity is one of nature's most fascinating quantum processes. It was discovered over a hundred years ago in mercury cooled to the temperature of liquid helium (about -452°F).

Since the discovery of superconductivity in mercury, the phenomenon has also been observed in other very low-temperature materials. The materials include many metals and a niobium-titanium alloy that can quickly turn into wire. The absence of electrical resistance in superconducting wires means they can tolerate very high electrical currents, but above a "critical current", the electron pairs break up, and superconductivity is demolished. Technologically, the wires have opened up new applications for superconductors, including windings to create strong magnets. In the 1970s, scientists used superconducting magnets to generate the high magnetic fields required to develop magnetic resonance imaging (MRI machines). Most recently, scientists have introduced superconducting magnets to guide electron beams in synchrotrons and accelerators in scientific user facilities. In 1986, scientists discovered a new class of copper oxide materials that showed superconductivity but at temperatures far higher than metals and metal alloys. These materials are referred to as high-temperature superconductors. Although they are cooled, they are superconducting at much warmer, some of them at temperatures higher than liquid nitrogen.

1.1 HOW DOES SUPERCONDUCTIVITY WORK?

These cold superconductors usually work by allowing electrons to overcome their usual aversion to each other and get closer to each other. to form Cooper pairs. The certainty of each electron's identity decreases in this low energy state. This allows electrons to slip through the atoms with ease.

The definition of superconductor can be given as a material that includes the superconductivity as part of its physical properties. Normally, as the temperature of a conductor decreases, its conductivity increases as it approaches absolute zero. However, superconductors are special materials whose resistance drops to zero and

maximum conductivity is reached after a certain critical temperature.

This is an important point to consider when defining what a superconductor is and when explaining the definition of a superconductor. At this point, when the temperature drops below the critical temperature, the superconductor's conductivity is maximized and the material also undergoes complete emission of the magnetic field flux.

There are two types of superconductors. They are called Type I and Type II superconductors. Type I superconductors make a sudden transition from normal to superconducting at transition temperature and vice versa. These superconductors exhibit a complete Meissner effect below the transition temperature.

However, there is no sudden change in Type II. Instead, it first shows a partial Meissner effect and later a full Meissner effect between the two critical values of the applied magnetic field. Especially in the design of suspended trains, it has a wide range of uses for the Meissner effect.

1.2 PROPERTIES OF SUPERCONDUCTORS

The electrical properties produced by unique and special physical properties play an important role because they are superconductors that do not have such interesting electrical properties. One of these properties is the zero electrical DC resistance present in the material. It is a common property of all superconductors, regardless of the material's properties, such as heat capacity and critical temperature (because it can vary from material to material). Also, as defined above, the phenomenon of superconductivity results in a significant reduction in temperature.

All superconducting materials work the same. The critical temperature varies with the material, but when the temperature drops below the critical temperature, the resistance drops to absolute zero. In this way, the superconductivity of superconductors is a thermal property, indicating that the phenomenon after reaching the superconducting state has nothing to do with the material's physical properties.

When material changes from a non-superconducting state to a superconducting state, the physical properties of the material, which are the characteristics of the phase transition, change significantly. A magnetic field trigger occurs when the temperature drops below the thermal superconductor.

However, when an external magnetic field exceeds the critical magnetic field, the superconductor exits the superconducting state. It begins to behave like a regular conductor. This change in the phase of the superconducting material is caused by a difference in the Gibbs free energy.

In the superconducting phase, the free energy of the conductor is lower than the free energy of the normal non-superconducting phase. When a finite amount of free energy is supplied to the superconductor from an external magnetic field, the free energy of the superconductor increases squarely. It reaches the typical value of free energy. Therefore, a phase transition from the superconducting phase to the non-superconducting phase occurs in the conductor.

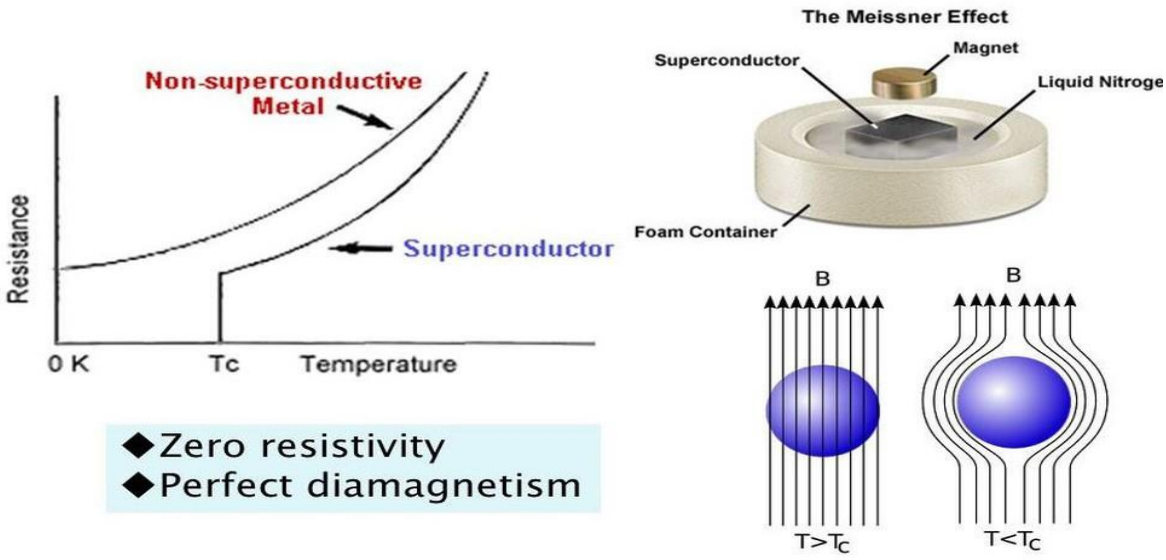

Figure 1.1 Diagram showing superconductivity and Meissner effect

1.3 Thermal Properties of Superconductors

The thermal properties of superconductors are very different from those of ordinary electrical conductors. Some electrons in a conductor are not bonded to individual atoms but are free to move around in the material. That is, their movement represents an electric current. However, these so-called conduction electrons are scattered by impurities, dislocations, particle boundaries, and lattice vibrations.

However, in superconductors, order between the conduction electrons prevents this scattering. Therefore, the current can flow without resistance. The placement of the electrons is called copper pairing. It includes the momentum of the electron, not the position of the electron. The energy per electron associated with this order is

minimal.

1.4 Applications of Superconductors

Superconductors are known to have zero DC electrical resistance. Therefore, most applications of the superconductor example are based on their properties and have the following advantages: B. Low power loss due to low energy loss, high-speed operation with zero resistance and continuous current, and high sensitivity. Examples of superconductors are:

- Mercury superconductors.
- Niobium-tin superconductors.
- Lanthanum-valium-cuprate superconductors.
- Yttrium-valium-cuprate superconductors.

Examples of applications for superconductors include medical MRI / NMR devices, magnetic energy storage systems, motors, generators, transformers, computer components, and sensitive instruments for measuring magnetic fields and currents.

CHAPTER 2
LITERATURE REVIEW

This literature review mainly includes researchers' numerical and experimental works on alternating current losses in the various structural arrangement of HTS cables.
S.Gijoy, K. E Reby Roy (2022) performed the finite element electromagnetic Network analysis and simulation of the 14-wire HTS Roebel cable. The result will be compared next. Another task of using H-formulation techniques to model the problem. However, some numerical simulations were performed. It was done to optimize the HTS Roebel cable, but no FEA work on the complete 3D structure of the Roebel cable has been done yet. Therefore, this work can be seen as the initiator of the electromagnetic 3D finite element analysis of the HTS Roebel cable.

S.Gijoy, K. E Reby Roy (2022) In this study, the influence of geometric parameters on the electromechanical stability of Roebel cables has been carefully studied using the 3D finite elements tool. Parameters include inner fillet radius, outer fillet radius, Robel angle, strand width, etc. First, the geometry is modelled, and its electromechanical simulation is performed for different loads conditions. Then all the parameters of the Roebel cable are changed in this standard geometry. After each variation, electromechanical simulation is performed for each set, and their effects are compared with the default geometry. Changed the distance between the stacks of strands in the crossing section and the straight section, The effect on mechanical stability and electromagnetic properties is observed.

S.Gijoy, K. E Reby Roy (2022) simulated the performance of Roebel strands for external tensile loads using 3D finite Elemental analysis (FEA) and geometric importance. Examined mechanical stability parameters for Roebel cables and compared the results with other work. The study was performed on a monolithic Roebel strand. We have concluded that the typical twist of a strand is one Important parameter that should not be ignored during the optimization label cable. Therefore, the voltage induced in the Roebel strand cancels it. External loads do not depend solely on geometric parameters, not only for the typical twist of the strands.

J Yang et al., (2022) In this article, we will first create a 3D finite element model of a CORC cable. It includes complex geometries, angle dependence of critical currents, and periodic settings. Modelling is validated by measurements performed on the transport loss of a two-layer CORC cable. Subsequently, the simulation results show that the primary transport loss shifts from the former to the superconductor with increasing current. On the other hand, the loss seen in the outer layer is more significant than in the inner layer due to the shielding effect between the layers. It also leads to the current non-uniformity of CORC cables.
In contrast to the two-layer case, the eddy current loss of the copper former is always dominant without cancelling the reverse winding layer. Hence, the simulated single-layer structure shows stronger frequency dependence. Single-structured core eddy currents are denser on the outside. Finally, AC transport loss is compared between pure HTS tape, double-layer cable, and single-layer cable. It has been confirmed that it has a two-layer structure that minimizes loss. It means that even placements can better use cable space and superconducting materials. This work is an essential reference for the structural design of the CORC cable, as it has shown the electromagnetic behaviour inside the CORC cable.

V A Anvar et al. (2018) demonstrate 3DSSS detailed FE modelling of CORC® wire under bending stress. A multi-layer CORC® bending test conducted by Advanced Conductor Technologies LLC experimentally validated the FE model. The elastoplastic properties of the individual tape composites and their temperature dependence are considered. A critical intrinsic tensile strain value of 0.45% is assumed to be the threshold at which the performance of individual tapes is irreversible. The proposed FE model correctly describes the bending test of CORC® wire and can be used to investigate other types of loads. Parametric research using dependent variables is underway to pursue further optimization of CORC® cables and wires for a variety of applications.

Y Wang et al. (2018) present a thorough study of CORC cables by combining experimental and numerical methods. In particular, the focus is on understanding how cable structures affect magnetization loss and how they can reduce it. The novelty of this paper lies in the use of the new T-A formulation, which was used first in the 3D modelling of real-world CORC cables. Using the new T-A formulation of finite

element software, it is possible to investigate how winding directions and multi-layer structures affect the magnetization loss of CORC cables. In addition, the effects of CORC cable banding are being studied as an effective way to reduce losses. Striped ribbon CORC cables have significantly reduced magnetization loss at high magnetic fields compared to cables without stripes. At low magnetic fields, banding increases the loss when the number of filaments is low and decreases as the filaments continue to grow. Still, this loss reduction is much lighter than at high magnetic fields. This paper can provide an efficient tool for studying the electromagnetic behaviour of CORC cables and offer valuable tips for designing CORC cables. Minimize the loss of high-energy physics and energy transformation applications.

M Solovyov et al. (2014) experimentally and theoretically studied the AC loss in transport and magnetization of single-layer ReBCO cables. The cable tested consisted of five parallel spirally wound coated conductor strips on a round core. The pitch is 40 mm, the complete doubling is six times, and the total length of the cable is 24 cm. The transport loss was measured using a transport current with a maximum amplitude of 600A at 36Hz and 72Hz. Alternate magnetic fields of up to 50 mT are applied. Measurement of magnetization loss at 36Hz and 72Hz. The achieved excellent agreement between the experimental results and the simulation of magnetization loss. However, the experimental results of transport loss are significantly larger than the predictions obtained from the simulation. Nevertheless, they are lower than the theoretically assumed transport AC loss of straight superconducting tapes with the same critical current.

N Amemiya et al. (2014) studied the 3D structure of the Roebel cable made of coated conductors affects the operation of AC loss. AC power loss measurements and numerical analysis of electromagnetic fields were performed using a 6-wire Roebel cable and several reference conductors. One straight sheath conductor, a 3x1 stack with three straight sheath conductors stacked, and a 3x2 stack. Here, two 3x1 stacks are placed next to each other. They compared AC losses of the Roebel cable and the reference conductor to each other. The discussed AC loss characteristics were d based on the electromagnetic phenomenon inside the superconductor obtained from the numerical electromagnetic field analysis. The verified effect of the 3D structure of the

Roebel cable on the AC loss characteristics is based on experimental and numerical results.

P Layes et al. (2013) studied the effect of orientation and magnetic field strength. U (I) measurements of several commercial CCs were carried out in our JUMBO facility in a free bore of 100 mm and magnetic field up to 10 T at 4.2 K and 77 K. we can adjust the angle between the applied field and the average vector to the tape between 0 and 180°. The resulting *U* (I) curves were approximated by various mathematical models using Matlab software, and from these, the parameters describing the angular dependence of the critical current, *I*c, were determined. The produced three-dimensional surface plots of *I* c as a function of angle and field strength and a suitable fit found. Then extrapolated, the fitting process was up to 30 T to determine the superconductor's behaviour in the high field region.

F Grilli et al. (2013) provide a literature review of calculating AC loss for HTS tapes, wires, and equipment. Technical superconductors have relatively complex shapes (filaments or layers that can be twisted or transposed) and are composed of various materials. It causes multiple losses. This article calculates the contribution of such losses, such as hysteresis loss, eddy current loss, coupling loss, and ferromagnet loss. It also provides estimates of losses incurred in various power applications.

C Barth et al. (2011) investigated various shapes of Roebel cables mechanically and electrically. First, the shapes of different meandering structures were analyzed using a 3D finite element method (FEM) model to evaluate resistance to tensile loads and possible minimum dislocation lengths. Next, we used FEM simulation to investigate the electromagnetic properties of the 2D cross-section of the Roebel cable. Improvements in the meandering structure were derived from these simulations. It allows for approximately the same twist pitch but improves the mechanical stability and current capacity of the entire cable assembled with Roebel.

V Lombardo et al., (2010) studied various aspects such as 2D current density uniformity and YBa {sub-2} Cu {sub-3} O {sub-7- {Delta}} coated conductor certification and minimum requirements related to the manufacturing process. It is shown. ROEBEL cable. Test results obtained with superconducting transformers for

critical current measurements of liquid helium are presented, discussed and single YBa {sub-2} Cu {sub-3} O {sub7- {Delta}} coated conductors. Compared to the performance of the strip.

W T Norris et al. (1978) described two methods for calculating the hysteresis loss of a rigid superconductor. The London model is envisioned, and the critical current density is assumed to be magnetic field independent. It can see that the loss of insulated wires of different cross-sections is considered, but for wires of different shapes with the same current capacity, the loss of a single wire can fluctuate up to 3 times. Saturation recent loss is typically 0.4-0.6Ic 2μ0 / π.

The loss at the edge of the thin sheet is also calculated, and the fourth power dependency on current (for low current) is found. Three systems have been studied: wide sheet current parallel slits (similar to Lc, equal to μ0j2g2π3F4 / 24), two wide strip edge pairs lying back-to-back and carrying antiparallel currents (similar to Lc, equivalent to μ0πj2s2F4). / 6), and one extended thin wall parallel to the current flow on a vast sheet (identical to Lc, equal to μ0π3j2a2F4 / 3). Lc is the loss per cycle per unit length, F is the peak current as a percentage of saturation current, g is the slot width, s is the strip spacing, a is the height of the unevenness, and j is the critical current per unit width. Density. All MKS unit systems.

CHAPTER 3
OBJECTIVES

The literature review shows that the research works are conducted through numerical analysis of the high-temperature superconducting structures. Only the experimental results on the comparative studies of various HTS cable structures are limited.
The primary objective of this study is to obtain a more quantitative insight into the alternating current losses of various HTS cable structures at liquid nitrogen temperature.

- To determine the electrical losses on various structural arrangements of high-temperature superconducting cables.
- To compare the AC losses and efficiency of different structural formats of HTS cables.

CHAPTER 4
METHODOLOGY

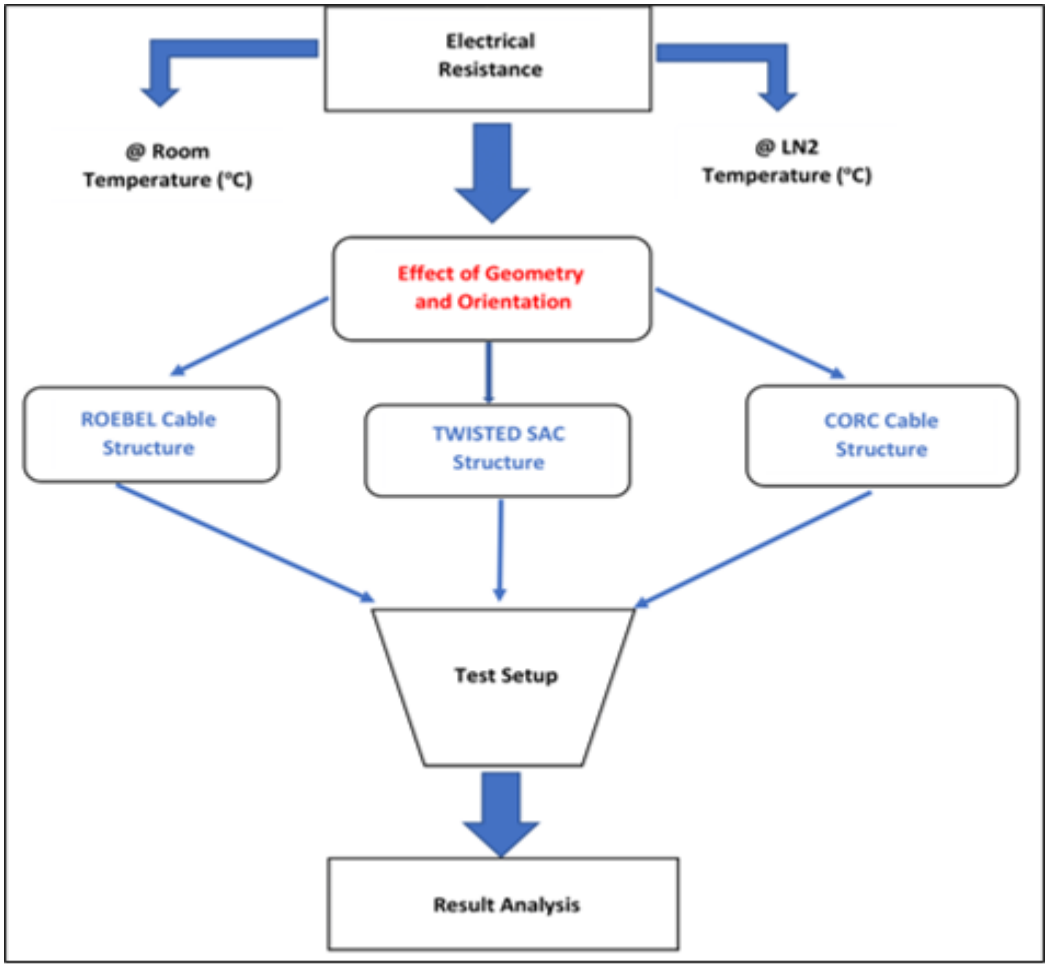

The major problem in designing an electrical circuit is the low resistance of the specimen at liquid nitrogen temperature; thus, the first step is to determine the electrical resistance of the model at the liquid nitrogen temperature.

Resistance is measured at both liquid nitrogen, and room temperatures are measured.

The HTS cable structures and orientation to be studied at the liquid nitrogen temperature are identified (Roebel cable structure, CORC cable structure and twisted sac structure), and the designs are to be made.

Then the electrical circuit design is to be made to measure the values of electrical current and voltage passing through the various structures at liquid nitrogen temperature.

A set-up is made to measure the values using the circuit designed, and the values are to be experimentally measured .and further numerical calculations are done to find the alternating current losses in the specimen at liquid nitrogen temperature.

Then the experimental results are to be analyzed to conclude which structural arrangement is more efficient under the given conditions.

CHAPTER 5

MEASUREMENT OF ELECTRICAL RESISTANCE OF SPECIMEN

5.1 PROCEDURE

- The resistance measurement is carried out with Kelvins Double bridge
- The specimen is connected to a wire of diameter 2.5sq mm using the brazing process.
- The model is immersed in a liquid nitrogen bath at 77K and atmospheric pressure.
- The leads are connected to the kelvins double bridge and from where we can find the resistance.

5.2 DIMENSIONS OF THE SPECIMEN (COPPER STRIP)

Length	63 mm
Breadth	2 mm
Thickness	0.5mm

Table 5.1 Dimensions of the Test Specimen

5.3 SPECIMEN PREPARATION

The copper is brazed to the 2.5 sq mm wire using brazing process and only brazing can be done join the specimen with the wire as other methods will build more resistance in the specimen other than material resistance. Then this brazed specimen is immersed in the liquid nitrogen bath for the testing .

Figure 5.1 a) Brazing of specimen b) brazed specimen

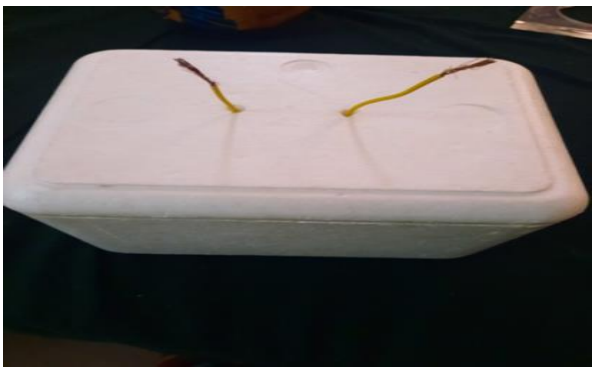

Figure 5.2 Test Setup for measuring the resistance of specimen at LN2 temperature

5.4 WORKING OF KELVINS DOUBLE BRIDGE

The Kelvin Bridge or Kelvin Double Bridge is a modified version of the Wheatstone bridge that can accurately measure resistance values in the range 1-0.00001 ohms. It was named because it uses a different set of ratio arms and galvanometers to measure unknown resistance values.

Wheatstone bridges are used to measure resistance above 1 ohm, but when measuring resistance below 1 ohm, the leads connected to the galvanometer measure the resistance of the galvanometer device., Resistance is added. As the number of leads increases, there will be discrepancies in the actual resistance measurement. Therefore, a modified bridge called the Kelvin bridge can be used to solve this problem.

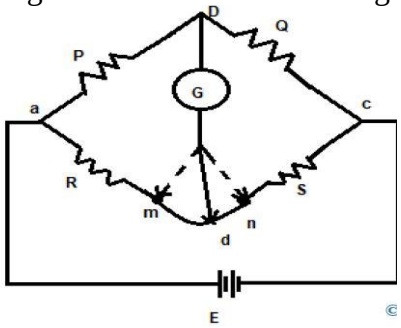

Figure 5.3 Kelvins Double Bridge circuit

Figure 5.4 Connections of specimen at LN2 temperature to kelvins double bridge

5.5 RESISTANCE MEASURED ON TEST SPECIMEN

SL NO.	SPECIMEN TYPE	RESISTANCE
1	Wire with copper strip in liquid nitrogen	11.8 milli ohm
2	Wire without copper strip in liquid nitrogen	11.6 milli ohm
3	Wire with copper strip at room temperature	15.8 milli ohm
4	Wire without copper strip at room temperature	16.2 milli ohm

Table 5.2 Readings from Kelvins Bridge

5.6 CALCULATION OF RESISTANCE USING MEASURED VALUES

The resistance measurements can be done using the equations for the series connection of the resistances.

As the connection are in series, resistance will be.

$$R = R_1 + R_2$$

$$11.8 = 11.6 + R_2$$

$$R_2 = 11.8 - 11.6$$

$$R_2 = 0.2\ m\Omega$$

R_1 =resistance of specimen at LN2 temperature with the strip
R_2 =resistance of specimen at LN2 temperature without strip

For CORC cables, R=0.37 m Ω

For twisted stack cables, R= 1.7 m Ω

5.7 VOLTAGE CALCULATION

$$V = IR$$

$$v = 0 \cdot 4 \times 0 \cdot 2 \times 10^{-3}$$

$$v = 0 \cdot 6 \times 10^{-3}\text{V}$$

CHAPTER 6
STRUCTURAL ARRANGEMENTS TO BE STUDIED

6.1 ROEBEL CABLE STRUCTURES

The Roebel bar was invented by Ludwig Roebel in 1912 to reduce the eddy currents of large generators. The 2Roebel bar consists of insulating copper strands that intersect in a spiral rod. A similar concept is used for superconducting conductors (RAC) assembled in Roebel. In this task, we call it a Roebel cable for brevity. Roebel strand

The cable is made by cutting a REBCO-coated conductor into a meandering shape. The cutting pattern is shown in Figure 6.1. The shape of the pattern is defined by the parameters of straight cross-section width w_s, cross-section width w_c, dislocation length `t, cross-section angle α, and internal radius Rin. The pattern repeats at each dislocation length.

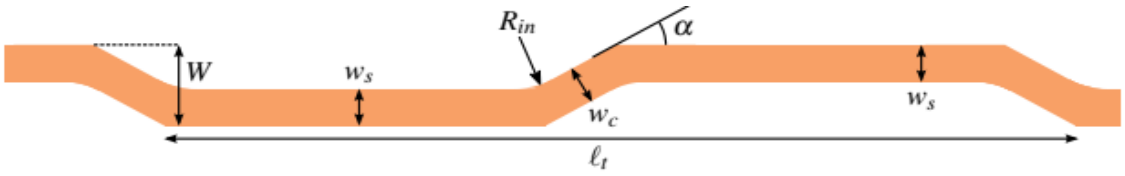

Figure 6.1 Structural dimensions [Simon J et al.,]

PARAMETERS	DIMENSIONS(MM)
W	4
w_s	1.9
w_c	1.9
α	30°
l_t	116
R_{in}	1

Table 6.1 Dimensions of Roebel cable structure

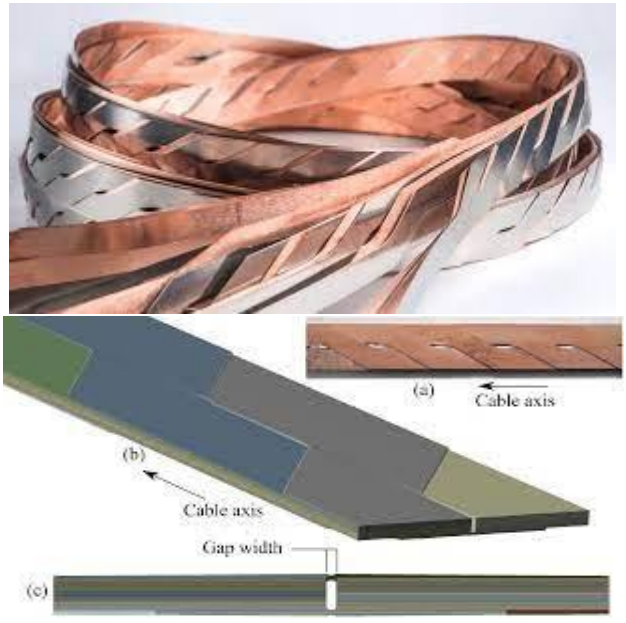

Figure 6.2 Roebel cable arrangement[W. goldacker et.al]

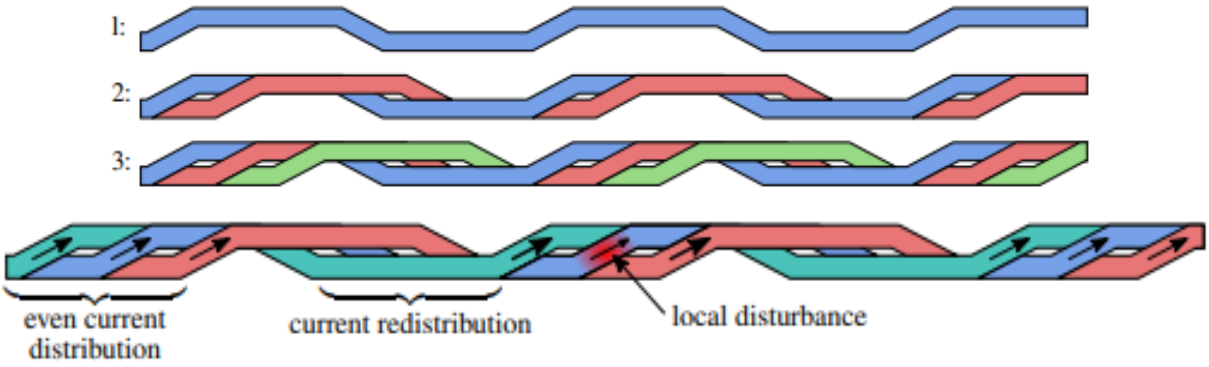

Figure 6.3 Assembly of a Roebel cable with three strands. [J.simon et.al]

Several punch strands are built into the Roebel cable. Strands will be added Individually by spirally wrapping them around the cable. This is done for short cables by hand. For longer cables, a semi-automatic cable assembler is used. assembly. This process is shown in Figure 6.3. The strands of the assembled cable are completely twisted, this means that each core will move all positions in the cable in the same way. When fully displaced, the path length of each strand will be the same when the cable is bent. This makes the Roebel cable easier to bend than a non-intersecting stack. Complete transportation It also ensures that each strand has the same self-inductance and mutual inductance in other strands. As the current increases, the current distribution becomes uniform. Between the strands. This is suitable for applications where field quality is important like Accelerator magnet.

6.1.1 STRUCTURES FOR EXPERIMENTATION

Figure 6.4 Roebel structure for experimental study A and B) 2 stranded cable c)1 stranded cable D) 3 stranded cable

The Roebel cable structure is cut into the dimensions using laser cutting technology using the CAD diagram made with the dimensions in the table. As the dimensions should be accurate. These strands are then arranged into the Roebel structure using hand as the length of the strands are small.

Figure 6.5 Laser cutting of copper

6.2 CORC CABLE STRUCTURE

HTS cables were initially designed to be relatively large Frame or core with a diameter of 40 mm or more Bi-2223 tape and subsequent REBCO coated conductor. I was injured. I needed a big former to prevent this Winding elongation to reach the irreversible yield point of the buy 2223 tape, 0.2% to 0.4% lower than the axial direction Only about -0.1% under tension and pressure. The size of the former did not change after these cables Made from REBCO coated conductor instead of Bi- 2223 ribbons, but these highly elastic conductors Withstands extremely high winding loads. High elasticity of REBCO lower layer Due to axial compression The HTS cable that ultimately led to the concept of CORC® cable. Instead of REBCO tape with supermarket the conductive film faces outward and exposes the film axially. Tension load with REBCO tape wrapped Superconducting film facing the former. This orientation Apply axial pressure to the REBCO film. Compressive elongation that allows at least -1.25% elongation in advance Mechanical deterioration will occur.

Figure 6.6 A 3 mm wide superconducting tape containing a 30 μm thick substrate wound onto a 2.8 mm diameter former. A 3 mm wide copper tape is wound in parallel to the superconducting tape to ensure a constant winding angle close to 45.[[D C van der lan et.al]

Figure 6.7 CORC cable arrangement a) Original arrangement b) Orientation for numerical studies [M solovyov et.al] c)Arrangement for experimental studies[D C van der lan et.al]

6.2.1 STRUCTURE FOR EXPERIMENTATION

Figure 6.8 Arrangement of CORC cable structures -2 mm copper sheet winded on 3 mm diameter brass rod at 45 degree

PARAMETERS	DIMENSIONS (mm)
Width of copper sheet	2
Diameter of rod	3
Thickness of sheet	0.5
Angle of winding	45
Pitch	5.3mm
Length	11cm,22cm,33cm

Table 6.2 Dimensions of CORC cable structure

6.3 TWISTED STACK CABLE STRUCTURE

Another concept motivated by the study of fusion magnets was presented by MIT. The idea is to solder three stacks of twisted CC to a grooved copper rod. This cable design is called Twist Stack Tape Cable (TSTC) and is shown in the figure. So far, this concept has been plagued by the thermal stress of composites. The process of assembling a long, thick stack has not yet taken place.

Figure 6.9 Twisted arrangement [J yang et.al]

6.3.1 ARRANGEMENT FOR TESTING

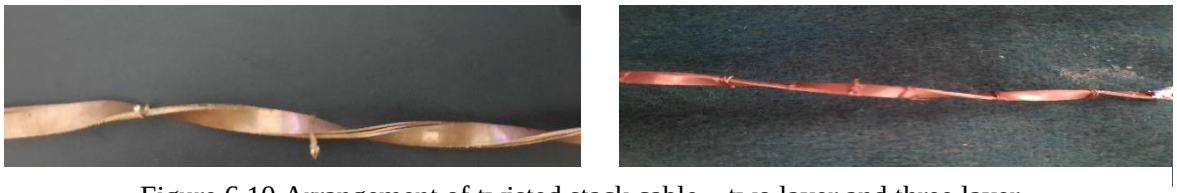

Figure 6.10 Arrangement of twisted stack cable – two layer and three layer

CHAPTER 7
DESIGN OF THE CIRCUIT TO MEASURE THE CURRENT AND VOLTAGE

At liquid nitrogen temperature (77 K) the resistance of the specimen is very low thus the voltage to be supplied to the HTS specimen should be very low or else short circuit will happen and which will burn out the circuit thus the major hindrance for the designing of the circuit is to find a source of voltage which can be used. then the other problem is to find out the range of the ammeter and voltmeter to be used.

7.1 DESIGNED CIRCUIT

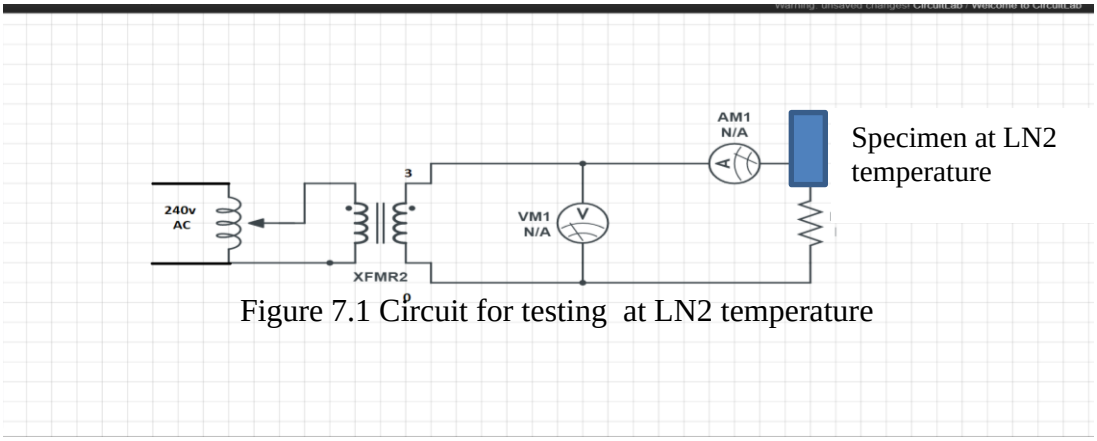

Figure 7.1 Circuit for testing at LN2 temperature

The circuit consist of,

1. A rheostat

   To adjust the input voltage of 220 v, in the range of 0- 220 v.

2. A step-down transformer

   For stepping down the input voltage in the range of 0 to 3 v

3. Milli ammeter

   Which is connected in series with the circuit to measure the current flowing through it in milli ampere range.

4.Milli voltmeter

To measure the voltage across the specimen. which is connected in parallel with the circuit.

According to the resistance found out the ammeter and the voltmeter for the range is selected. Gradually a voltage is applied through the various structural arrangement through a transformer where the input voltage of 230V is stepped down to 0-3V.The values of the current and voltage is noted. Final calculations for finding the AC losses are done.

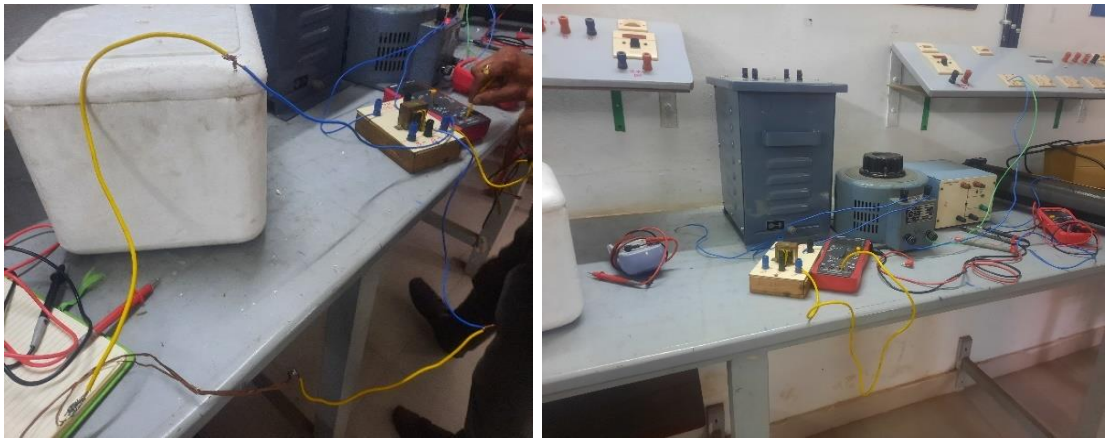

Figure 7.2 Setup for measurement of current flowing through the various structures at cryogenic temperature

7.2 THEORETICAL CALCULATION OF CURRENT

For Roebel Cables,

$$I = \frac{v}{R}$$

$$\text{AT, } v = 0.3 \times 10^{-2} v$$

$$R = 12 \cdot 19 \times 10^{-3} \Omega$$

$$I = 0.3 \times 10^{-2} / 12.19 \times 10^{-3}$$

$$\text{I=0.24 A}$$

$$\text{AT V= } 0.2 \times 10^{-2} v$$

$$I = 0.2 \times 10^{-2} / 12.19 \times 10^{-3}$$

$$\text{I=1.6 A}$$

7.3 EXPERIMENTAL VALUES FOR ROEBEL CABLE STRUCTURES

VOLTAGE	CURRENT AT LN2 TEMPERATURE	CRRENT AT ROOM TEMPERATURE
0.3*10^-2	0.15	0.09
0.5*10^-2	0.26	0.22
1*10^-2	0.42	0.39
2*10^-2	0.89	0.76

Table 7.1 Measured value for 3 stranded roebel structure

VOLTAGE	CURRENT AT LN2 TEMPERATURE	CURRENT AT ROOM TEMPERATURE
0.3*10^-2	0.12	0.09
0.5*10^-2	0.25	0.2
1*10^-2	0.41	0.39
2*10^-2	0.86	0.78

Table 7.2 Measured value for 2 stranded roebel structure

VOLTAGE	CURRENT AT LN2 TEMPERATURE	CURRENT AT ROOM TEMPERATURE
0.3*10^-2	0.19	0.15
0.5*10^-2	0.22	0.2
1*10^-2	0.39	0.35
2*10^-2	0.81	0.78

Table 7.3 measured value for 1 stranded roebel structure

7.4 EXPERIMENTAL VALUES FOR CORC CABLE STRUCTURE

VOLTAGE(mV)	CURRENT AT LN2 TEMPERATURE	CURRENT AT ROOM TEMPERATURE
0.3	0.1	0.01
0.5	0.15	0.09
1	0.33	0.23
2	0.64	0.58

Table 7.4 Experimental values for CORC cable structure (11 cm) 1 winding

VOLTAGE(mV)	CURRENT AT LN2 TEMPERATURE	CURRENT AT ROOM TEMPERATURE
0.3	0.06	0.05
0.5	0.13	0.13
1	0.22	0.22
2	0.55	0.51

Table 7.5 Experimental values for CORC cable structure (22cm) 1 winding

VOLTAGE(mV)	CURRENT AT LN2 TEMPERATURE	CURRENT AT ROOM TEMPERATURE
0.3	0.12	0.1
0.5	0.16	0.14
1	0.33	0.26
2	0.54	0.5

Table 7.6 Experimental values for CORC cable structure (22cm) 2 winding

VOLTAGE(mV)	CURRENT AT LN2 TEMPERATURE	CURRENT AT ROOM TEMPERATURE
0.3	0.08	0.07
0.5	0.2	0.15
1	0.38	0.31
2	0.69	0.54

Table 7.7 Experimental values for CORC cable structure (33cm) 2 winding

VOLTAGE(mV)	CURRENT AT LN2 TEMPERATURE	CURRENT AT ROOM TEMPERATURE
0.3	0.1	0.08
0.5	0.16	0.11
1	0.29	0.27
2	0.6	0.59

Table 7.8 Experimental values for CORC cable structure (33cm) 3 winding

7.5 EXPERIMENTAL VALUES FOR TWISTED STACK CABLES

VOLTAGE(mV)	CURRENT AT LN2 TEMPERATURE	CURRENT AT ROOM TEMPERATURE
0.3	0.08	0.08
0.5	0.12	0.14
1	0.32	0.3
2	0.62	0.58

Table 7.9 Twisted stack cable with 2 layer

VOLTAGE(mV)	CURRENT AT LN2 TEMPERATURE	CURRENT AT ROOM TEMPERATURE
0.3	0.16	0.08
0.5	0.3	0.17
1	0.58	0.33
2	0.65	0.59

Table 7.10 Twisted stack cable with 3 layer

7.6 CALCULATION OF AC LOSSES IN THE STRUCTURES

As the experiments are done at 50 hz frequency and at low voltages the AC losses consist of only power losses. which we can found oyt with help of the mathematical equations .

Thus power loss for each strands are calculated,

SAMPLE CALCULATION,

$$\boldsymbol{power\ loss} = \text{AC}\ \boldsymbol{losses}$$

$$\boldsymbol{P = I^2 \times R}$$

$$\boldsymbol{V = 0.3 \times 10^{-2}}$$

$$\mathbf{I = 0.19\ A}$$

$$\boldsymbol{R = 12.19 \times 10^{-3}}$$

$$\boldsymbol{P = 0.19^2 \times 12.19 \times 10^{-3}}$$

$$\boldsymbol{P = 0.4 \times 10^{-3} W}$$

VOLTAGE(mV)	0.3	0.5	1	2
3 STRAND ROEBEL(mW)	0.24	0.824	2.049	7.8
2 STRANDED ROEBEL(mW)	0.175	0.76	2.15	7.99
1 STRANDED ROEBEL(mW)	0.4	0.58	1.85	9.65
CORC (33CM)3WINDING(mW)	0.12	0.316	1.039	4.44
CORC(33cm)3 winding(mW)	0.079	0.4949	1.78	5.88
Twisted 2 layer(mW)	0.077	0.175	1.245	4.67
Twisted 3 layer(mW)	0.31129	0.175	1.245	4.67
CORC (22cm) 2 winding(mW)	0.179	0.3164	1.346	3.604
CORC (22cm)1 winding(mW)	0.0449	0.2088	0.598	3.7389
CORC (11cm)1winding(mW)	0.1236	0.2781	1.346	5.0625

Table 7.11 Calculated AC losses for each structure

CHAPTER 8
RESULTS

8.1 VOLTAGE-CURRENT CURVES FOR ROEBAL STRUCTURE

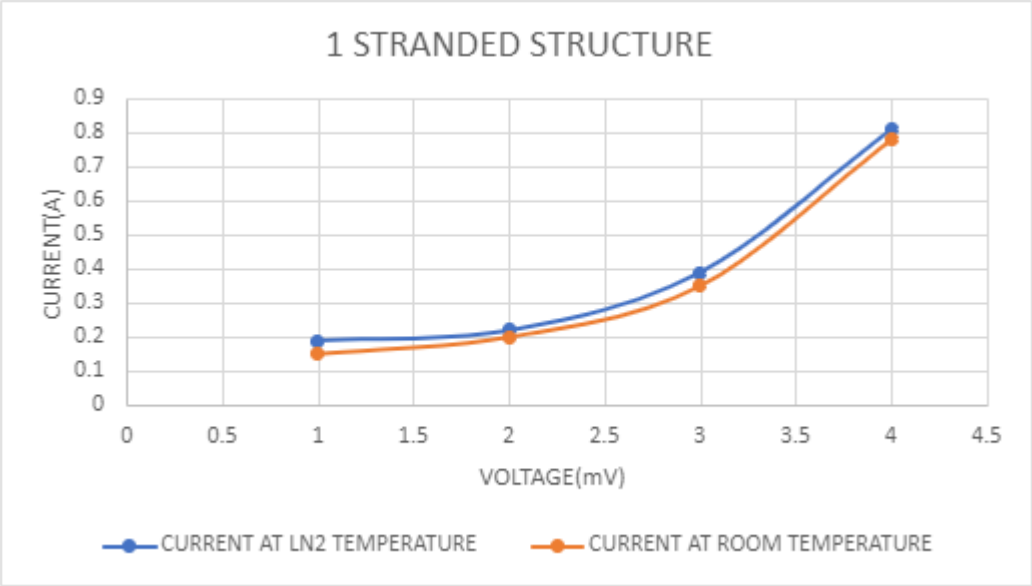

Figure 8.1 V-I curve for one stranded structure

Figure shows the variation of current values through the one stranded Roebel cable structure. from the graph we can identify that for one stranded structure the increase in current is not that much appreciable.

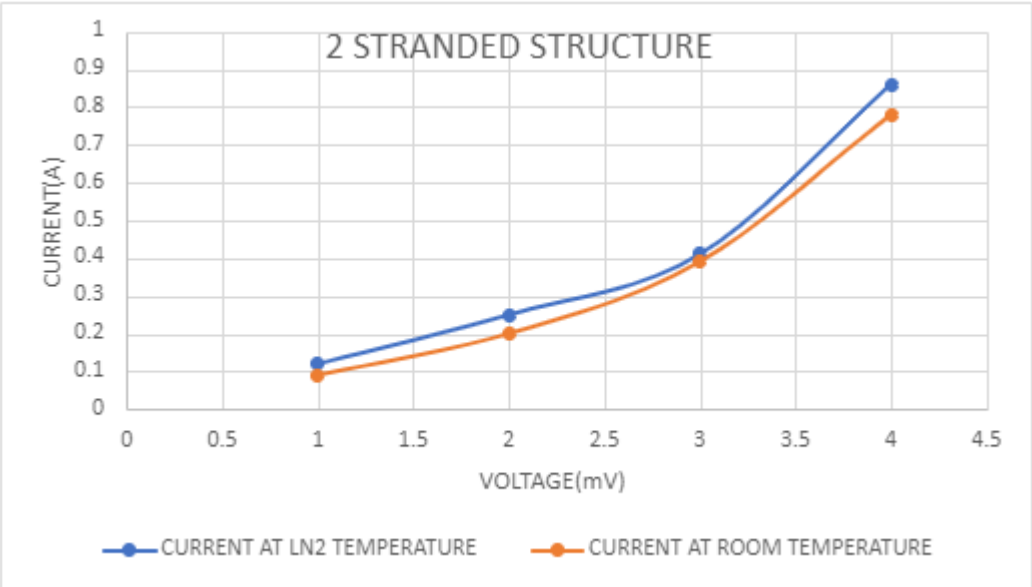

Figure 8.2 V-I curve for two stranded structure

Figure shows the value of rise of the current in the two stranded Roebel cable structure in two stranded structures only at high voltages there is a considerable change in the current value at the liquid nitrogen temperature.

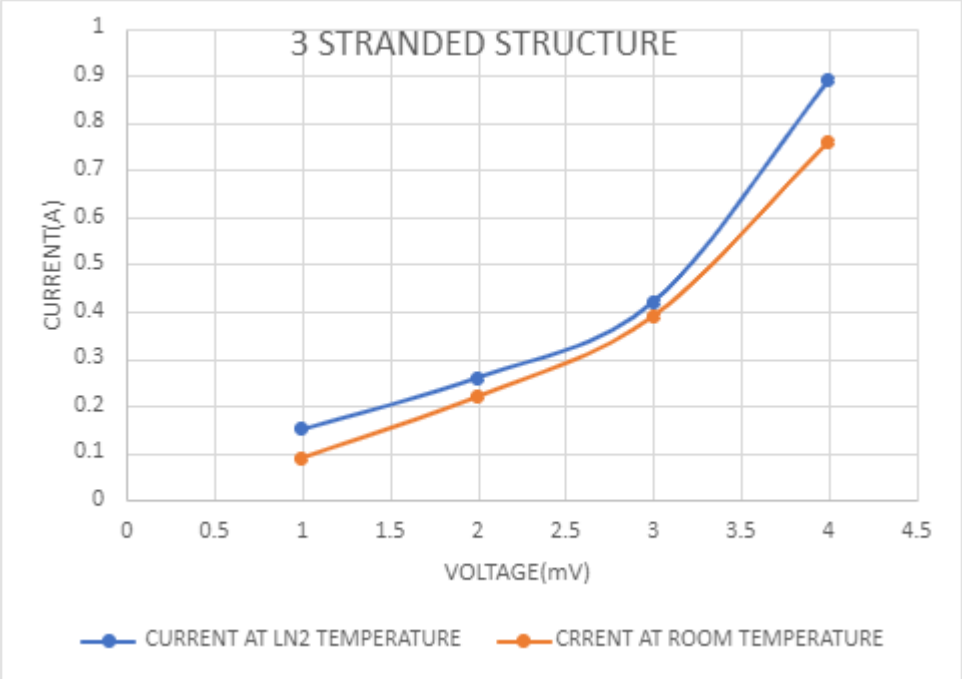

Figure 8.3 V-I curve for three stranded structures

Figure shows the variation of current values with voltage at liquid nitrogen and the room temperature for three stranded Roebel structures.in three stranded structures we can identify that at all voltages the rise of current value at liquid nitrogen temperature is very much appreciable.

8.2 COMPARISON OF THEORETICAL VALUE OF CURRENT AND EXPERIMENTAL VALUES

Theoretical value of current(A)	Experimental values of current(A)		
	1 strand	2 strand	3 strand
0.24(at 0.3mV)	0.19	0.12	0.15
0.41 (at 0.5mV)	0.22	0.25	0.26
0.82 (at 1mV)	0.39	0.42	0.41
1.6 (at 2mV)	0.86	0.81	0.89

Table 8.1 Values of current and voltage measured compared to theoretical values

The above table shows that the value we got in the experimental setup is much lower compared to the theoretical value this is because of the electrical losses happening in the circuit at liquid nitrogen temperature.

8.3 VOLTAGE-CURRENT CURVES FOR CORC CABLE STRUCTURES

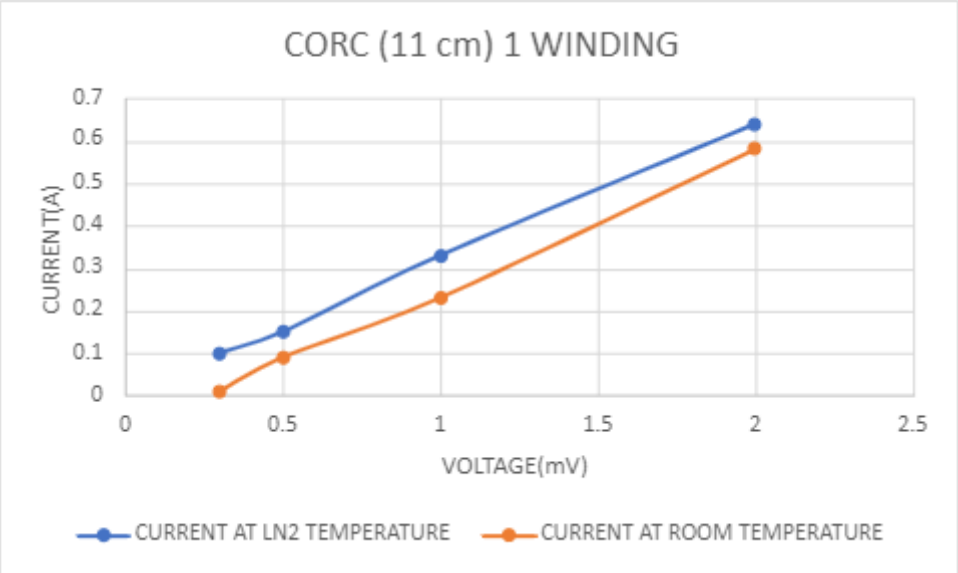

Figure 8.5 V-I curve for CORC cable(11cm) one winding structure

Figure shows current voltage variation through the CORC cable structure (11 cm) one winding.at liquid nitrogen temperature the structure shows a high increase in the current value.

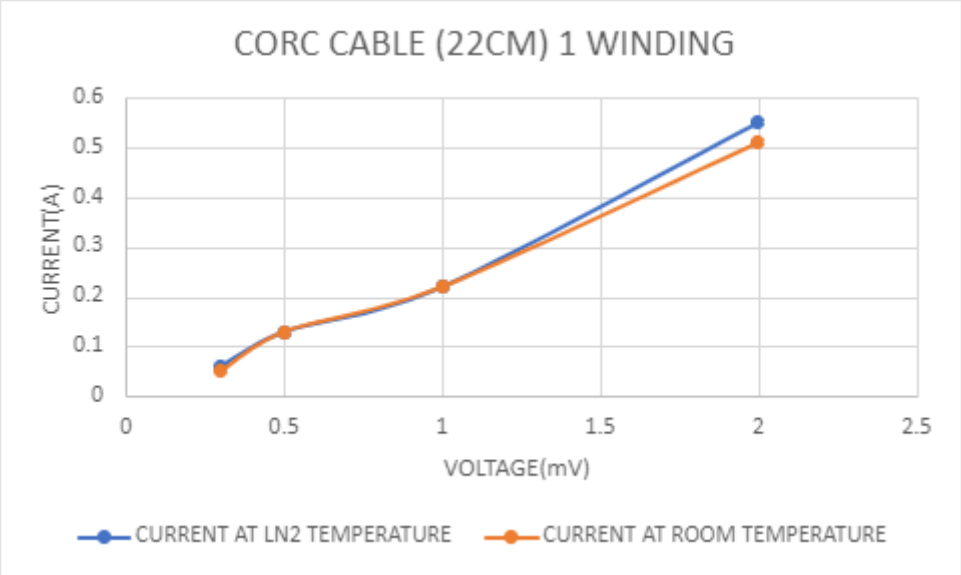

Figure 8.6 V-I curve for CORC cable(22cm) one winding structure

Figure shows the variation of the current and voltage at liquid nitrogen and at room temperature for 22 cm long one winding CORC cable structure. This structure doesn't have any appreciable change in the current at liquid nitrogen temperature.

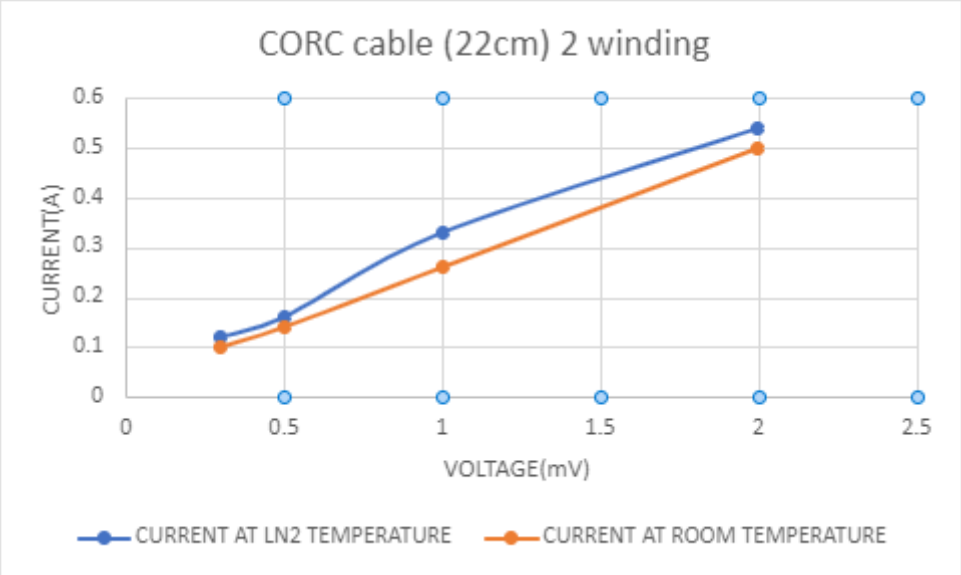

Figure 8.7 V-I curve for CORC cable(22cm) one winding structure

Figure shows the variation of V-I with the reduction of temperature to liquid nitrogen temperature. It's having an increase of current flowing at intermediate voltages only i.e., between 0.5V. and 1 V.

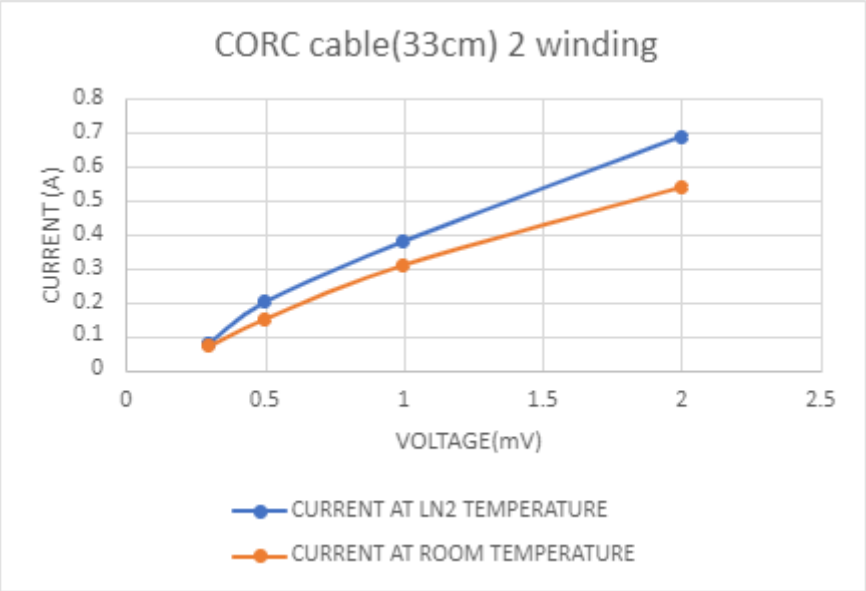

Figure 8.8 V-I curve for CORC cable(33cm) two winding structure

Figure shows the variation of current and voltage at liquid nitrogen temperature for the CORC cable 2 winding structure. its showing a great increase in the value of current as the voltage supply increases.

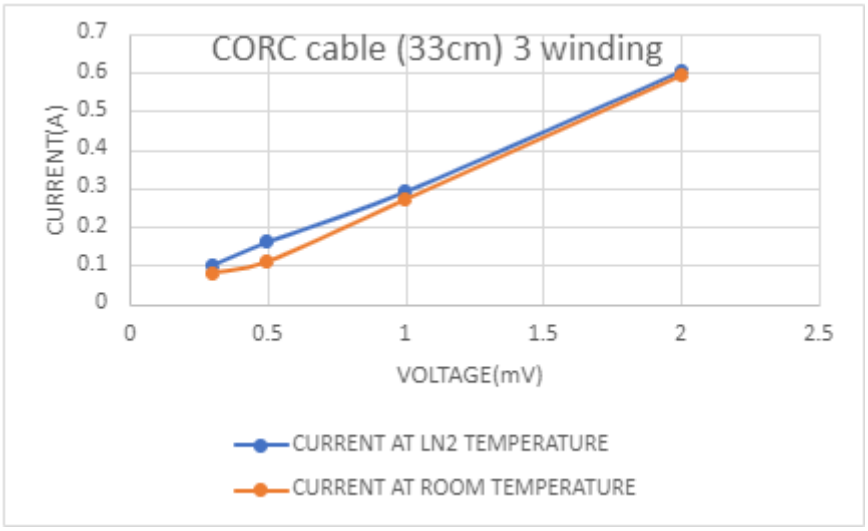

Figure 8.9 V-I curve for CORC cable(33cm) three winding structure

The figure shows that when a third winding is added to the CORC cable structure the resistance will be increasing at liquid nitrogen temperature also thus there is no change in the current flowing through the cable structure.

8.4 VOLTAGE-CURRENT CURVES FOR TWISTED STACK CABLE STRUCTURES

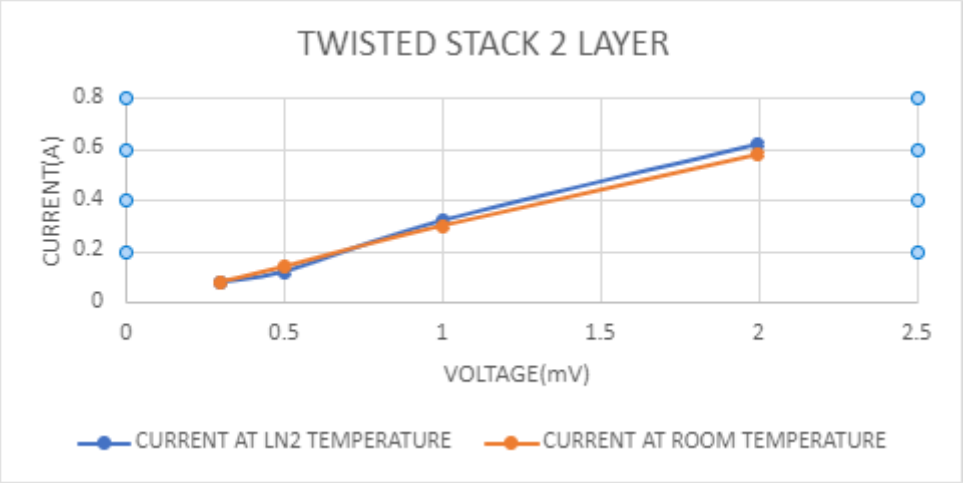

Figure 8.10 V-I curve for Twisted stack cable 2 layer structure

Figure shows that there is no considerable change in the current for a two layered twisted stack cable structure this is due to the mor resistance buildup in the structure due to the arrangement and orientation of the structure.

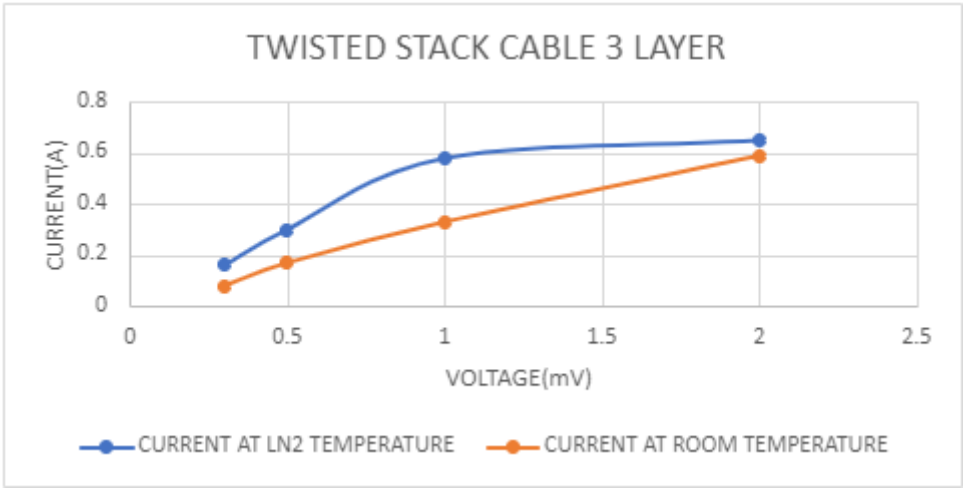

Figure 8.11 V-I curve for Twisted stack cable 2-layer structure

Figure shows that the 3-layer twisted stack structure is no that much effective at high and lower voltage ranges in liquid nitrogen temperature.

8.5 COMPARISON OF VOLTAGE-CURRENT CURVES OF VARIOUS STRUCTURES

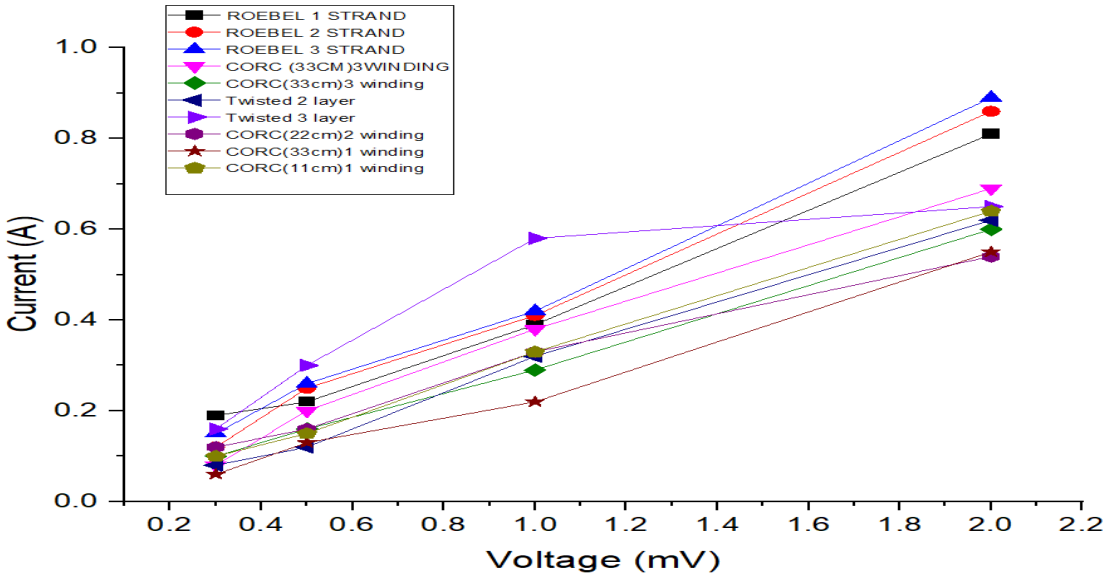

Figure 8.12 comparison of current flow through all the 10 structures studied

The figure 8.12 shows that except for twitwisted three layered structure all other structure has a very good rise in the current flowing through it as the voltage rises.and when comparing the structural arrangement roebal cable with 3 strand has the maximum capacity of current carrying.and CORC cable with three windings have lower current carrying capacity.

8.6 COMPARISON OF AC LOSSES OF VARIOUS STRUCTURES

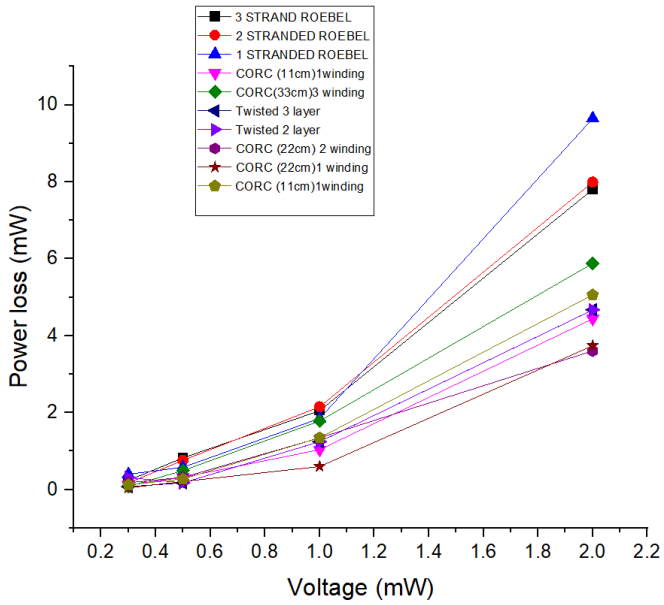

Figure 8.13 Comparison of AC losses for all the 10 structures

From figure it is clear that the AC losses is very high in the one stranded Roebel cable structure compared to all other structure when using in high voltages. At low voltage values the AC current losses is almost same for all the structures. Then at the high voltages the CORC cable structure with two winding is efficient. But in all the voltage ranges the CORC cable structure with one winding is more efficient.

CHAPTER 10

CONCLUSION

Experimental study on the superconducting cable structures at liquid nitrogen temperature was performed. The experimentation was done to find out the value of current flowing through the superconducting structures at liquid nitrogen temperature .and to calculate the AC losses through various structures. the result indicated that the as we performed experiments at 50 hz and low voltages the AC losses through the structures is only due to the power losses happening inside the circuit. The results indicates that the twisted stack cable structure with two layer is having the maximum current carrying capacity at liquid nitrogen temperature.

When comparing the results of the AC losses through structures the CORC structures with winding at 45° with a 2mm wide copper strip on 3mm diameter brass wire is having less AC losses comparing to the other structures .this is due to the arrange of the copper strip over the surface of the brass rod ,the winding angle which is a major area of the contact resistance in the structure so when winding in 45° the resistance due the structure ,orientation ,the contact of the air etc are limited.

Thus, from this experimental we can give an inference that the CORC cable structures are more efficient when comparing the Roebel cable structures and twisted stack structures which we taken for the experimentation.

REFERENCES

- Frank, R. Heller, W. Goldacker, A. Kling, C. Schmidt. (2008). Roebel assembled coated conductor cables (RACC): Ac-Losses and current carrying potential, *J. Phys.Conf. Ser. 97 ,012147,*

- C. Barth, K.P. Weiss, M. Vojenčiak, S. Schlachter .(2011). Electro-mechanical analysis of Roebel cables with different geometries, *Supercond. Sci. Technol. 25 025007.*

- D.C. Van Der Laan. (2009) .YBa2Cu3O7-δ coated conductor cabling for low ac-loss and high-field magnet applications, *Supercond. Sci. Technol. 22 065013,,*

- Jiabin Yang, Chao Li ,Mengyuan Tian, Shuyu Liu, Boyang Shen, Luning Hao, Yavuz Ozturk, Tim Coombs.(2022). Analysis of AC Transport Loss in Conductor on Round Core Cables, *Journal of Superconductivity and Novel Magnetism 35:57–63*

- N. Amemiya, T. Tsukamoto, M. Nii, T. Komeda, T. Nakamura, Z. Jiang.(2014). Alternating current loss characteristics of a Roebel cable consisting of coated conductors and a three dimensional structure, *Supercond. Sci. Technol. 27 ,035007.*

- N. Amemiya, T. Tsukamoto, M. Nii, T. Komeda, T. Nakamura, and Z. Jiang. (2014).Alternating current loss characteristics of a Roebel cable consisting of coated conductors and a three-dimensional structure, *Supercond.Sci. Technol., vol. 27, no. 3, Art. no. 035007.*

- S. Gijoy, K.E.Reby Roy. (2020) .3D Finite Element Electromagnetic Analysis of a 14-Strand HTS Roebel Cable., *J. Supercond. Nov. Magn. 33 1709– 1719.*

- S. Gijoy, K.E.Reby Roy. (2020) . The importance of geometrical parameters on the mechanical stability of Roebel cables., *J. Supercond. Nov. Magn. 33 1709–1719.*

- S. Gijoy, K.E.Reby Roy. (2020) .Influence analysis of the geometrical parameters on the electro-mechanical stability of HTS Roebel cables., *J. Supercond.Nov. Magn. 33 1350–6307.*

- T. Tsukamoto, T. Mifune, Y. Sogabe, Z. Jiang, T. Nakamura, N. Amemiya. (2015). Influence of geometrical configurations of HTS Roebel cables on their AC losses,*IEEE Trans. Appl. Supercond. 25 4802005.*

- W. Goldacker, F. Grilli, E. Pardo, A. Kario, S. I. Schlachter, and M.Vojenˇciak, 2014, Roebel cables from REBCO coated conductors: A one-century-old concept for the superconductivity of the future, *Supercond.Sci. Technol., vol. 27, no. 9, Art. no. 093001.*

- W. Ta, Y. Liu, K. Wang, L. Liu, and Y. Gao. (2019). “Effect of the twisting chirality configuration on the electromechanical behavior of multilayer superconducting tapes,” *Phys. Lett. A, vol. 383, no. 10, pp. 949–956*